Preclinical Studies of Vorinostat (Suberoylanilide Hydroxamic Acid) Combined with Cytosine Arabinoside and Etoposide for Treatment of Acute Leukemias

Ken Shiozawa,[1,4] Takeo Nakanishi,[1,3] Ming Tan,[2] Hong-Bin Fang,[2] Wen-chyi Wang,[2,5] Martin J. Edelman,[1] David Carlton,[1] Ivana Gojo,[1] Edward A. Sausville,[1] and Douglas D. Ross[1,3]

Abstract

Purpose: Vorinostat [suberoylanilide hydroxamic acid (SAHA)] is a potent histone deacetylase inhibitor with promising clinical efficacy as an anticancer agent. In this preclinical study, we evaluated combining cytosine arabinoside [1-β-D-arabinofuranosylcytosine (ara-C)] and/or etoposide with vorinostat for use in the treatment of acute leukemias.

Experimental Design: Cell survival was examined *in vitro* in HL-60 human myeloid leukemia cells and K562 myeloid blast crisis chronic myelogenous leukemia cells, using the 2,3-bis[2-methoxy-4-nitro-5-sulfophenyl]-2*H*-tetrazolium-5-carboxanilide inner salt and/or fluorescein diacetate/propidium iodide assays. Drug interactions were analyzed by the combination index method (CalcuSyn) and by a novel statistical method that we developed (SynStat). Cell cycle phase distribution was measured by flow cytometry.

Results: Cytotoxic antagonism resulted when vorinostat was combined concomitantly with ara-C; however, when vorinostat was given first followed by a drug-free interval before ara-C treatment, this sequential combination was mostly synergistic. Etoposide combined with vorinostat was additive to synergistic, and the synergism became more pronounced when etoposide was given after vorinostat. Cell cycle analyses revealed that the sequence-dependent interaction of vorinostat and ara-C or etoposide reflected the arrest of cells in G_1 or G_2 phase during vorinostat treatment and recovery into S phase after removal of vorinostat.

Conclusions: These findings using two independent methods to assess drug combination effects provide a preclinical rationale for phase I trials of the sequential combination of vorinostat followed by ara-C and etoposide in patients with advanced or refractory leukemias. CalcuSyn findings were concordant with those of SynStat, validating the use of the latter in analyzing drug interactions.

Leukemia is one of the 10 leading causes of cancer deaths in the United States (1); survival of adults with relapsed and/or refractory leukemias remains unsatisfactory. Although a few patients may achieve durable survival with chemotherapy or allogeneic bone marrow transplantation, the majority will not have the latter option available due to older age, absence of a donor, or refractory/progressive disease. Salvage therapy with regimens such as cytosine arabinoside [1-β-D-arabinofuranosylcytosine (ara-C)] and anthracyclines or ara-C and etoposide may induce remission only in 25% to 30% of these patients, but responses are usually of short duration. Thus, lack of effective therapy mandates development of new approaches to improve the outcome for adults with relapsed and refractory leukemias.

Vorinostat [suberoylanilide hydroxamic acid (SAHA)] is a second-generation hydroxamic acid–based hybrid polar compound originally shown to be a potent inducer of differentiation in murine erythroleukemia cells at micromolar concentrations (2, 3). Subsequently, vorinostat was shown to be a strong inhibitor of histone deacetylase with direct binding to the catalytic site (2, 4) and, hence, entered a new class of

Authors' Affiliations: [1]Program in Experimental Therapeutics, University of Maryland Marlene and Stewart Greenebaum Cancer Center, and Division of Hematology and Oncology, Department of Medicine, University of Maryland School of Medicine; [2]Division of Biostatistics, University of Maryland Marlene and Stewart Greenebaum Cancer Center, and Department of Epidemiology and Preventive Medicine, University of Maryland School of Medicine; [3]The Baltimore Veterans Affairs Medical Center, Baltimore, Maryland; [4]Second Department of Internal Medicine, Nagasaki University School of Medicine, Nagasaki, Japan; and [5]Mathematical Statistics Program, Department of Mathematics, University of Maryland, College Park, Maryland

Received 6/20/08; revised 11/10/08; accepted 11/24/08; published OnlineFirst 02/17/2009.

Grant support: U.S. NIH grant CA106767 (M. Tan and H-B. Fang) and a VA Merit Review grant (D.D. Ross).

The costs of publication of this article were defrayed in part by the payment of page charges. This article must therefore be hereby marked *advertisement* in accordance with 18 U.S.C. Section 1734 solely to indicate this fact.

Note: Supplementary data for this article are available at Clinical Cancer Research Online (http://clincancerres.aacrjournals.org/).

Requests for reprints: Douglas D. Ross, University of Maryland Marlene and Stewart Greenebaum Cancer Center, Room 9-031, Bressler Research Building, 655 West Baltimore Street, Baltimore, MD 21201. Phone: 410-328-8095; Fax: 410-328-6559; E-mail: dross@som.umaryland.edu.

doi:10.1158/1078-0432.CCR-08-1587

Translational Relevance

Vorinostat is showing promise for therapy of human cancers. Clinical trials are planned in a number of centers combining vorinostat with antileukemia agents such as arabinoside [1-β-D-arabinofuranosylcytosine (ara-C)] and etoposide. Our findings show that concomitant administration of vorinostat and ara-C produces cytotoxic antagonism and should be avoided. Furthermore, we find that the antagonism of vorinostat and ara-C can be overcome by sequential use of vorinostat followed by ara-C. Similarly, for etoposide combined with vorinostat, we found that the cytototoxic efficacy of etoposide was enhanced using a sequential (vorinostat followed by etoposide) schedule as well. Our studies implicate depletion of S-phase cells caused by vorinostat blocking cells in the G_1 or G_2 phase of the cell cycle as the biological basis for the antagonism seen with the concomitant schedule. These studies debut the first preclinical application of the SynStat statistical method for assessing drug combination effects, and provide further validation of this novel method.

anticancer agents targeted at the aberrant activity of histone deacetylase implicated in a variety of cancers (5, 6). Vorinostat is currently Food and Drug Administration approved for the treatment of refractory cutaneous T-cell lymphomas. In view of its effects on growth arrest, differentiation, and/or apoptotic cell death documented in a wide range of transformed cells *in vitro* and in animals (6–12), vorinostat has become a focus of interest as a promising anticancer agent. Phase I/II trials have recently evaluated vorinostat as a single agent given either i.v. or orally to patients with diverse malignancies, including leukemias. These trials indicate that vorinostat had favorable oral bioavailability compared with other histone deacetylase inhibitors, had acceptable toxicity in heavily pretreated patients, and produced objective evidence of tumor regression (13–15).

Accumulating preclinical evidence suggests that vorinostat can potentiate the cytotoxicity of both conventional cytotoxic agents and novel molecularly targeted compounds. Vorinostat has been found to interact additively or synergistically *in vitro* with anthracyclines, etoposide, cisplatin (16), 5-fluorouracil (17), flavopiridol (18, 19), imatinib mesylate (9, 12), 5-azacytidine or decitabine (20), bortezomib (21), and all-*trans* retinoic acid (22). These findings raise the possibility of combining vorinostat with antileukemia agents because daunorubicin, idarubicin, and etoposide have significant therapeutic activity in acute myelogenous leukemia. However, to date, there are no published preclinical studies of the combination of vorinostat with ara-C, one of the most active agents for the treatment of acute myelogenous leukemia. One approach to increase the therapeutic efficacy of salvage therapy for leukemia is to combine ara-C and etoposide with novel agents such as vorinostat that may sensitize the cells to the cytotoxic activity of the salvage drugs.

A caution to this approach, however, is the possibility that the S-phase–blocking effect of vorinostat may antagonize the S-phase–dependent cytotoxicity of ara-C. Hence, in this preclinical study, we evaluated the cytotoxic interaction of vorinostat with ara-C or etoposide in human leukemia cell lines (HL-60 and K562). The cytotoxic interactions of concomitant or sequential administration of vorinostat with ara-C or etoposide were analyzed by the combination index (CalcuSyn; refs. 23, 24) and by the maximal power design (SynStat; refs. 25, 26) methods. The combination index method derives a specific parametric model by fixing the mixture ratio, whereas the maximal power design method is able to evaluate combinations across several concentration ratios. Additionally, because the cytotoxicity of ara-C and etoposide is affected by cell cycle phase (27–29), we investigated the effects of alterations in cell cycle phase distribution caused by vorinostat on the sensitivity of HL-60 or K562 cells to these antileukemia drugs.

Materials and Methods

Cell cultures

HL-60 cells were obtained from the American Type Culture Collection. K562 cells were generously provided by Dr. Yoshikazu Sugimoto of the Japanese Foundation for Cancer Research (Tokyo, Japan). Cells were cultured in RPMI 1640 (Biofluids) supplemented with 10% heat-inactivated fetal bovine serum (Gemini Bio-Products) at 37°C in a humidified atmosphere containing 5% CO_2. Cells in logarithmic growth phase between passages 5 and 20 were used for these experiments.

Compounds

The National Cancer Institute kindly provided vorinostat under a collaborative agreement between Merck and Co., Inc., and the Division of Cancer Treatment and Diagnosis, National Cancer Institute. Cytarabine (ara-C; Faulding Pharmaceutical Co.) and etoposide (Ben Venue Laboratories, Inc.) were obtained from the University of Maryland Medical Center Pharmacy and were reconstituted according to the instructions of the manufacturer. Stock solutions of 10 mmol/L vorinostat were prepared in DMSO and stored at -20°C until use.

Measurement of cell survival

Unless otherwise stipulated, the number of viable cells in culture was determined at the end of 72 h of drug (or control) exposure. Cells were seeded in 96-well plates at an initial concentration of 1×10^4/mL of culture, at a final volume of 200 μL/well, and were exposed to varying concentrations of vorinostat, ara-C, or etoposide, alone or in combination either simultaneously or sequentially with vorinostat given first followed by ara-C or etoposide. Cytotoxicity was assessed using the Cell Proliferation Kit II (Roche Applied Science), a colorimetric method for quantification of viable cells that is based on the cleavage of the tetrazolium salt 2,3-bis[2-methoxy-4-nitro-5-sulfophenyl]-2*H*-tetrazolium-5-carboxanilide inner salt (XTT) to form formazan dye by metabolically active cells, according to the protocol of the manufacturer. Following the appropriate exposure to drug(s), 50 μL of XTT solution were added. After 4-h incubation at 37°C, absorbance at 490 nm was measured using a microplate reader (DYNEX Technologies, Inc.). Cell viability was also assessed with the fluorescein diacetate/propidium iodide method by flow cytometry after staining with fluorescein diacetate and isotonic propidium iodide (Sigma-Aldrich) as described previously (30). The IC_{50} values were computed using CalcuSyn software (Biosoft).

Concurrent exposure to vorinostat with ara-C or etoposide

Cells were seeded into 96-well plates as described above, then treated with serial dilutions of each drug individually or with both drugs simultaneously at a fixed ratio of doses that corresponded to 0.125, 0.25, 0.5, 1, 2, 3, and 4 times the individual IC_{50} values. After 72 h of exposure, growth inhibition was measured using the XTT assay.

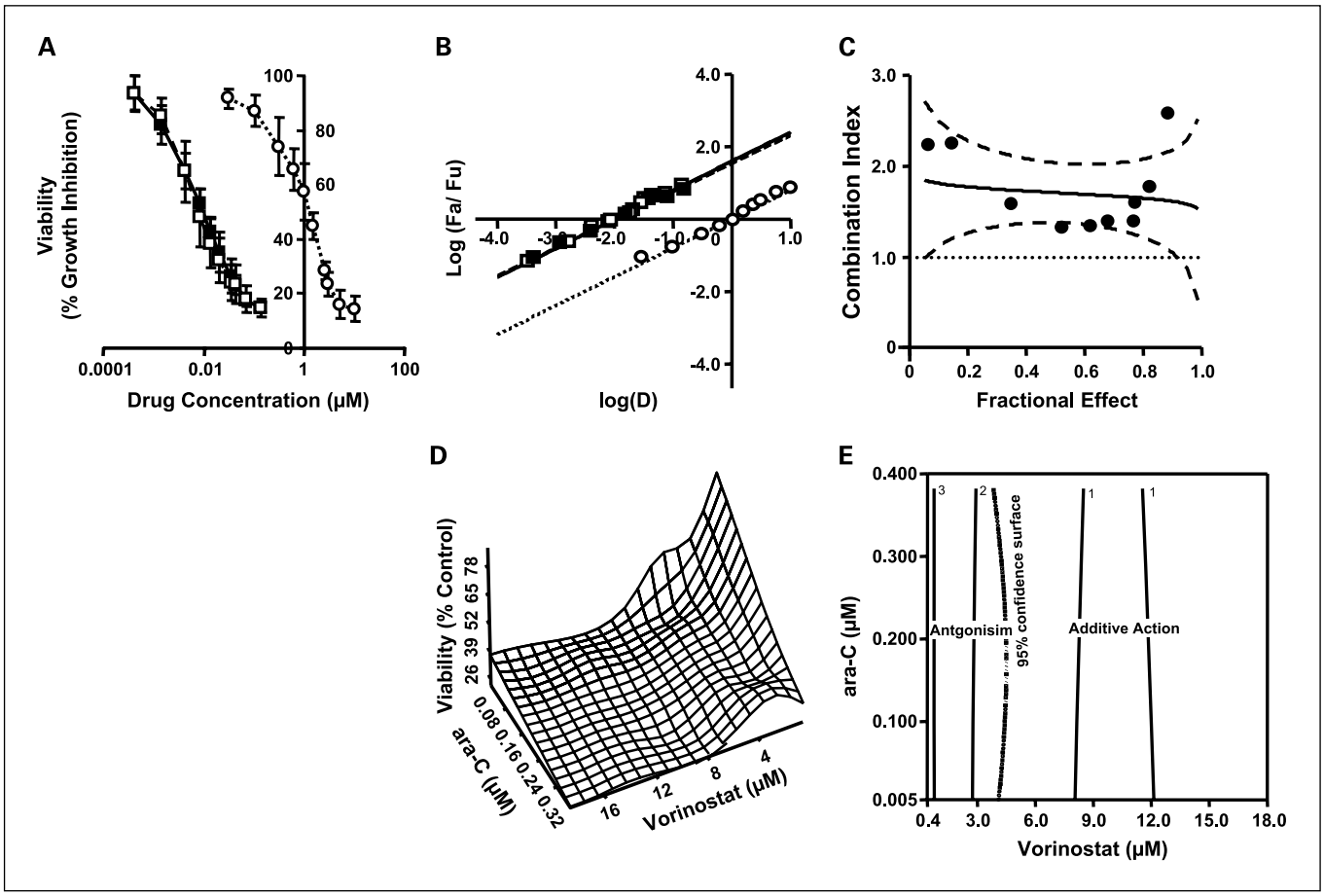

Fig. 1. Simultaneous combination of vorinostat and ara-C results in a less-than-additive or antagonistic interaction in HL-60 cells. *A,* dose-response curves for growth inhibitory activity of vorinostat alone (○), ara-C alone (□), or the combination (■; at a vorinostat/ara-C ratio of 72: 1). HL-60 cells were exposed for 72 h continuously to the designated concentration of drugs as described in Materials and Methods. Growth inhibition was measured using the XTT assay. Points, mean for three separate experiments (done on different days), with each experimental point done in duplicate (n = 6); bars, SD. *B,* CalcuSyn median effect plot for the interaction of the combination of vorinostat with ara-C shown in *A*. The resulting dose-response curves were averaged, and the fraction affected was calculated for each concentration and then entered into the software. Fa, affected fraction; Fu, unaffected fraction. *D,* concentrations of drug used (○, vorinostat alone; □, ara-C alone; ■, the combination). *C,* the combination index plots derived from CalcuSyn software. Dashed lines, 95% confidence intervals; dotted line, combination index = 1. *D,* SynStat maximum power design derived three-dimensional response surface, based on the experimental data from 18 simultaneous combinations of vorinostat and ara-C with four replicates at each combination in HL-60 cells. *E,* the contour plot of the estimated interaction index (τ) surface. The dotted line indicates the 95% confidence intervals for additivity.

Sequential exposure to vorinostat with ara-C or etoposide

HL-60 cells were exposed to seven different concentrations of vorinostat in T-25 flasks seeded at an initial cell density of 1×10^4/mL. After 24 h, vorinostat was removed by washing with PBS; then the cell pellet was resuspended in fresh, drug-free medium to achieve a final cell density of 1×10^4/mL; and 200 μL of this cell suspension were added per well of 96-well plates. After the specified period of culture in drug-free medium, ara-C or etoposide was added to the respective wells of the 96-well plates. At the end of 72 h of exposure to ara-C or etoposide, cytotoxicity was measured using the XTT assay or by counting cell numbers with a Coulter counter (Beckman-Coulter, Inc.) everyday for up to 9 d.

Interaction analysis

CalcuSyn method. To determine synergistic, additive, or antagonistic effects of the drug combinations, two methods of interaction analysis were used. The first was the combination index method of Chou and Talalay (23, 24). CalcuSyn software (version 2.0, Biosoft), which is based on this method and takes into account both potency [median dose (Dm) or IC_{50}] and the shape of the dose-effect curve (the m value), was used to calculate the combination index (CI). Synergy, additivity, and antagonism are defined as CI < 1, CI ± 1, and CI > 1, respectively. For this analysis, vorinostat and ara-C or etoposide were combined at fixed ratios as described above. The fraction affected and the corresponding combination index values were calculated for each concentration. Finally, the median effect method was used in the sequential combination studies to identify the most promising schedule of combinations. Triplicate data points were used for each concentration; each experiment was repeated at least twice (n = 6-9 replicates).

SynStat method. The SynStat version 1.beta software[6] is a statistics-based method that utilizes the maximal power design developed by Fang and Tan (25, 26). SynStat, written in the R programming environment, consists of three programs: SYN.design (to identify, based on dose-effect data for each of two drugs used alone, the most informative mixtures of the two drugs to be used in an experiment to assess the effect of the drugs in combination), SYN.test (for testing if there are significant departures from additivity in joint effect), and SYN.analysis [for further analyzing the nature of drug interactions (e.g., synergy or antagonism) and the concentrations of the drugs in the

[6] (http://www.umgcc.org/research/biostat.software.htm). The Readme document included with the software contains step-by-step instructions for installing and using the software, including a tutorial with sample data files.

combination at which these interactions appear]. Briefly, for each cell line, dose versus cytotoxicity data for each drug alone (vorinostat or ara-C or etoposide) were obtained. These data were then input into SYN.design, which obtained the dose-response curve of each single drug by regression analysis, as well as an estimate of the variance (e.g., the pooled variance from single drug data). SYN.design then specified the number of drug combinations, the doses for each drug in the combination, and the number of replicates to make in a given experiment so that the power of the F test to detect departures from the additive action of the two drugs is maximized. Then, cells were exposed to these multiple combinations of drug (11-19 combinations) for the time periods specified, and cytotoxicity was determined.

On completion of the drug combination experiments specified by SYN.design, the SYN.test program was used to test whether there was a significant departure from additivity (specified as a 15% difference in viability within the dose range of interest with a statistical power of 80% and a 5% significance level). When significant departures from additivity were found (i.e., $P < 0.05$), SYN.analysis was used to perform nonparametric regression analysis to estimate the dose-response surface, which shows the joint effects of the two-drug combinations.

To identify where synergism or antagonism relative to additivity occurs among the dose combinations, SYN.analysis also calculated the interaction index (τ) as proposed by Berenbaum, who extended the Lowe additivity model (isobologram; ref. 31), which is defined as follows:

$$\frac{x_A}{X_A} + \frac{x_B}{X_B} = \tau \qquad (A)$$

where, for a given effect level, x_A and x_B are the concentrations of drug A and drug B in the combination, and X_A and X_B are the concentrations of drug A and drug B given alone that achieve the same cytotoxic effect. For a given dose-effect level, X_A and X_B in Eq. (A) can be obtained from the single drug dose-response curves; x_A and x_B are obtained experimentally from the studies of drug A and drug B in combination. Hence, a τ value of 1 indicates additivity; $\tau < 1$ indicates synergy; and $\tau > 1$ indicates antagonism. Thus, given any drug combination and dose-effect level, an interaction index (τ) value can be calculated. With multiple combinations and dose-effect levels, a three-dimensional τ surface can be fitted to values of x_A and x_B, using a nonparametric method (25). To better display the dose-combination regions of additivity, synergism, and antagonism, the SYN.analysis program provides a contour plot of the interaction index (τ) surface plotted for values of x_A and x_B, where each contour line represents the same interaction index (τ) value labeled on the contour, and the dotted lines indicate the limits of the 95% confidence interval for additivity ($\tau = 1$).

Cell cycle analysis

Cell cycle phase distributions were estimated from cell nuclei stained with propidium iodide. Briefly, cells were exposed to concentrations of vorinostat (0.1-25 μmol/L) for the time periods indicated, washed with PBS twice, fixed with ice-cold 70% ethanol, and then stored at -20°C until the assay. RNA was destroyed with 0.2 mg/mL RNase A (Roche) and cell nuclei were stained with 0.05 mg/mL propidium iodide. Cell cycle phase distribution was estimated from flow cytometric data using the Modifit LT 3.0 flow cytometry modeling program (Verity Software House).

Results

IC_{50} values for vorinostat, ara-C, or etoposide as single agents. The sensitivity of HL-60 cells to vorinostat, ara-C, or

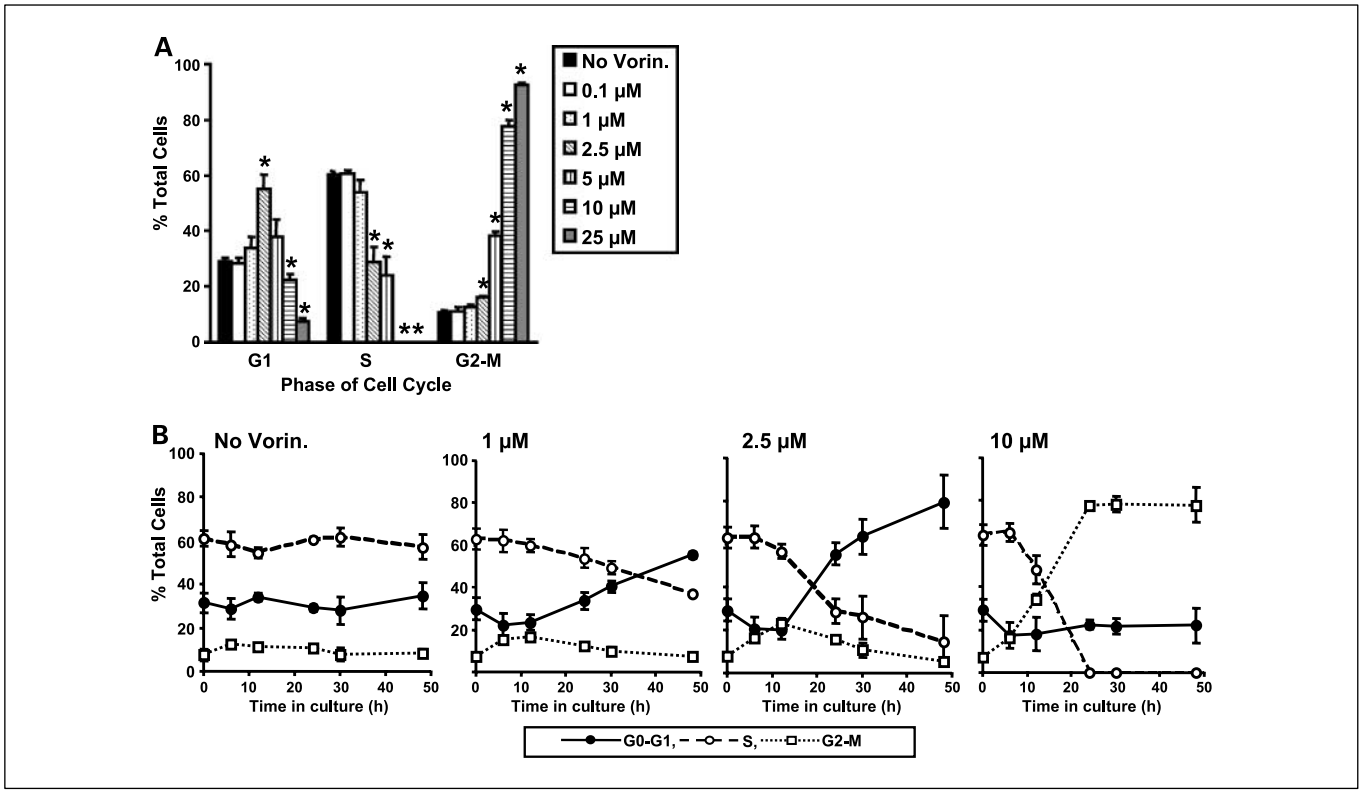

Fig. 2. Effect of vorinostat on the cell cycle phase distribution of HL-60 cells. *A,* effect of 24-h treatment with differing concentrations of vorinostat. Representative data of at least three separate experiments, done on different days. Statistical differences between untreated and treated samples at each cell cycle phase ($P < 0.001$) were determined using the two-sample t test. *B,* cells (2.5×10^5) were exposed to 0, 1, 2.5, and 10 μmol/L of vorinostat for the indicated hours, then subjected to cell cycle analysis as described in Materials and Methods. Points, mean of triplicate determinations; bars, SD.

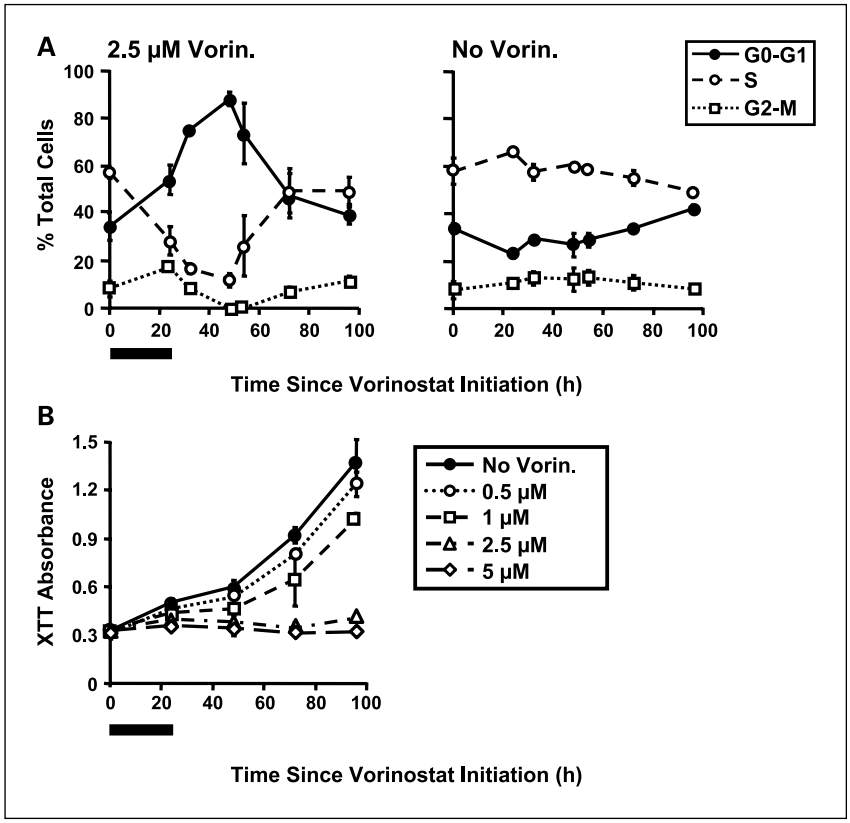

Fig. 3. Time course of recovery of cell cycle phase distribution or proliferation following exposure of HL-60 cells to 2.5 μmol/L vorinostat for 24 h. *A,* left, HL-60 cells (1×10^5/mL) were exposed to 2.5 μmol/L vorinostat for 24 h, vorinostat was withdrawn, and then cells incubated in drug-free medium for an additional 72 h. Cell cycle phase distribution was analyzed by flow cytometry at 0, 24, 32, 48, 54, 72, and 96 h after initial addition of vorinostat. Bar (*bottom left*), time of exposure to vorinostat. *Right,* as controls, cells were exposed to equivalent volumes of DMSO, then sampled at the time points indicated on the left. Points, mean of triplicates ($n = 3$) for each time point; bars, SD. *B,* cell proliferation after 24-h treatment with vorinostat. HL-60 cells (1×10^5/mL) cells were cultured in the presence or absence of the indicated concentrations of vorinostat for 24 h, vorinostat was removed by washing twice with PBS, and then the cells were incubated in drug-free medium. Cell proliferation was monitored daily for 4 d by the XTT assay. Bar (*bottom left*), time of exposure to vorinostat. Points, mean of triplicates for each point ($n = 3$); bars, SD.

etoposide after 72-hour exposure was determined by the XTT assay and by the fluorescein diacetate/propidium iodide method. The XTT assay IC_{50} values were (mean ± SD) 2.46 ± 0.54, 0.034 ± 0.015, and 0.29 ± 0.09 μmol/L for vorinostat, ara-C, and etoposide, respectively. The fluorescein diacetate/propidium iodide IC_{50} values were comparable to those obtained by the XTT method and were 1.46 ± 0.99, 0.016 ± 0.005, and 0.13 ± 0.06 μmol/L for vorinostat, ara-C, and etoposide, respectively.

For K562 cells, the XTT assay IC_{50} values after 96-hour exposure to drug were 0.16 ± 0.06, 0.008 ± 0.005, and 0.26 ± 0.18 μmol/L for vorinostat, ara-C, and etoposide, respectively.

Simultaneous combination of vorinostat and ara-C is additive or antagonistic. Because the ratio of XTT IC_{50} values for vorinostat and ara-C against HL-60 cells was 72:1, HL-60 cells were exposed to varying concentrations of vorinostat and ara-C simultaneously for 72 hours at a fixed ratio of 72:1 (vorinostat/ara-C), and then cell survival was measured by the XTT method. When data were analyzed by the CalcuSyn software, cytotoxic antagonism was observed (Fig. 1A-C), with combination index values significantly >1 for all fractional effect levels (Fig. 1C). For the fluorescein diacetate/propidium iodide method, the ratio of IC_{50} values (vorinostat/ara-C) was ~100:1. The combination of both drugs in the ratio of 100:1 also resulted in antagonism when cytotoxicity was measured by the fluorescein diacetate/propidium iodide method, reflecting our XTT assay data (Supplementary Fig. S1). Because the fluorescein diacetate/propidium iodide method is both time-consuming and laborious and because the XTT assay is semiautomated and offers a practical advantage over the fluorescein diacetate/propidium iodide method, we used the XTT assay for the majority of these studies.

Using SynStat software, 18 mixtures of ara-C and vorinostat were calculated that would be optimally informative. HL-60 cells were simultaneously exposed to these mixtures for 72 hours with four replicates at each mixture, and then cytotoxicity was measured by the XTT method. A three-dimensional response surface graph, generated from these data (Fig. 1D), represents the cell survival in the presence of the 18 mixtures of vorinostat and ara-C, with estimates of growth inhibition displayed for the entire dose range of combinations. With the observations from the combination experiments, the *F* test suggests that vorinostat with ara-C simultaneously against HL-60 is not additive [$F(3, 85) = 35.69$, $P < 0.0001$]. The contour plot of the estimated interaction index (τ) surface (Fig. 1E) provides a convenient means from which the joint action of vorinostat and ara-C can be assessed in terms of additivity, synergy, or antagonism. Unlike the CalcuSyn analysis, which detected only antagonism, SynStat analysis predicted additivity at any dose of ara-C when doses of vorinostat were relatively high (>6 μmol/L; Fig. 1E); cytotoxic antagonism was observed when the dose of vorinostat was relatively low, including the clinically tolerated range.

For K562 cells, the SynStat method predicted antagonism of vorinostat and ara-C at vorinostat doses <2 μmol/L, in agreement with that observed for HL-60 cells. At doses of vorinostat >2 μmol/L, additivity and possibly synergy are predicted in Supplementary Fig. S2A and B.

Vorinostat causes G_1-phase cell cycle arrest and decreases the proportion of S-phase cells. Vorinostat is known to block cells at the G_1 or G_2 boundary of the cell cycle at micromolar

concentrations (3, 5, 32). Because ara-C is an S-phase–specific agent (27), cell cycle phase distributions after exposure to vorinostat were examined to determine if cell cycle alterations could play an important role in the antagonistic interaction of vorinostat and ara-C. Cell cycle phase distributions were determined after 24-hour exposure to vorinostat in graded concentrations (0.1, 1.0, 2.5, 5.0, 10, and 25 μmol/L; Fig. 2A). These studies and a time course analysis (Fig. 2B) revealed that cells treated with vorinostat underwent G_1 phase arrest at lower (≤2.5 μmol/L) vorinostat concentrations and G_2-M phase arrest at concentrations >2.5 μmol/L (Fig. 2A and B). S-phase cells, in contrast, showed progressive depletion by increasing exposure time and/or concentration of vorinostat (Fig. 2).

Depletion of S-phase cells was reversible following removal of vorinostat (Fig. 3A). Treatment of HL-60 cells with 2.5 μmol/L vorinostat resulted in reduction of S-phase cells from 58% (pretreatment) to 28% after 24 hours of exposure. If vorinostat was removed at that point, S-phase entry remained blocked for an additional 24 hours; by 72 hours, the percentage of S-phase cells returned to pretreatment levels; however, the return to S-phase was not accompanied by cell division even after 96 hours (Fig. 3B, 2.5 μmol/L data).

Similar to HL-60 cells, 24-hour exposure of K562 cells to 2.5 μmol/L vorinostat depleted the percentage of S-phase cells from pretreatment levels of 53% to 13%; recovery of the percentage of S-phase cells to pretreatment levels occurred by 48 hours after the removal of vorinostat (see Supplementary Fig. S3). There were no significant changes in cell cycle phase distribution over these time points for cells not treated with vorinostat.

These findings suggest that diminished populations of S-phase cells caused by vorinostat may contribute to the antagonistic interaction of vorinostat and ara-C when combined simultaneously. Furthermore, the recovery of S-phase

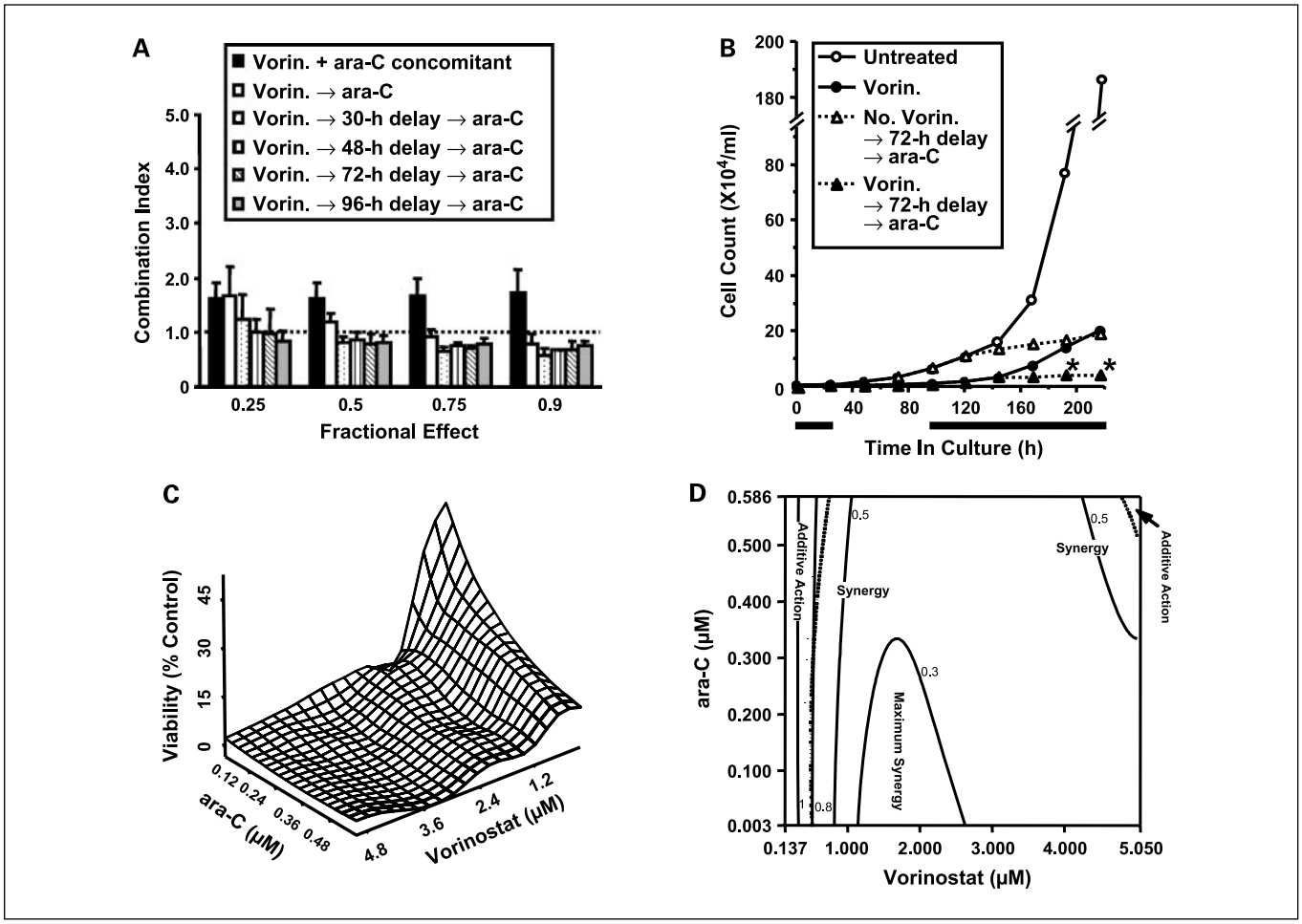

Fig. 4. The effect of sequence of administration on the interaction between vorinostat and ara-C. *A,* the combination indices for the interaction in relation to the fractional effect on HL-60 cells are shown for combinations using a 24-h pre-exposure to vorinostat followed by a 72- h exposure to ara-C starting at 0 h (*blank*), 30 h (*dot*), 48 h (*stripe*), 72 h (*border*), and 96 h (*shadow*) after vorinostat treatment. Columns, mean for three separate experiments done in duplicate ($n = 6$) in each treatment schedule; bars, SD. Dotted line, combination index = 1. *B,* cell proliferation assay. HL-60 cells (2.5×10^3/mL) were cultured in the presence or absence of 2.5 μmol/L vorinostat for 24 h, washed free of drugs, and incubated in drug-free medium for 72 h; aliquots of the cells were then treated with or without 34.7 nmol/L ara-C (at a molar ratio of vorinostat/ara-C of 72: 1) for an additional 72 h. Cell numbers were monitored daily for 9 d with a Coulter counter. Bar, time of exposure to vorinostat (*bottom left*) or time of exposure to ara-C (*bottom right*). Point, average value of two individual assays ($n = 2$). *, $P < 0.004$, significantly less than the values for cells treated with vorinostat alone with two-sample *t* test. *C,* SynStat maximum power design derived three-dimensional response surface, based on the experimental data from on the data from 18 sequential combinations of vorinostat and ara-C with five replicates at each combination in HL-60 cells. *D,* the contour plot of the estimated interaction index (τ) surface. The dotted lines indicate the limits of the 95% confidence interval for additivity.

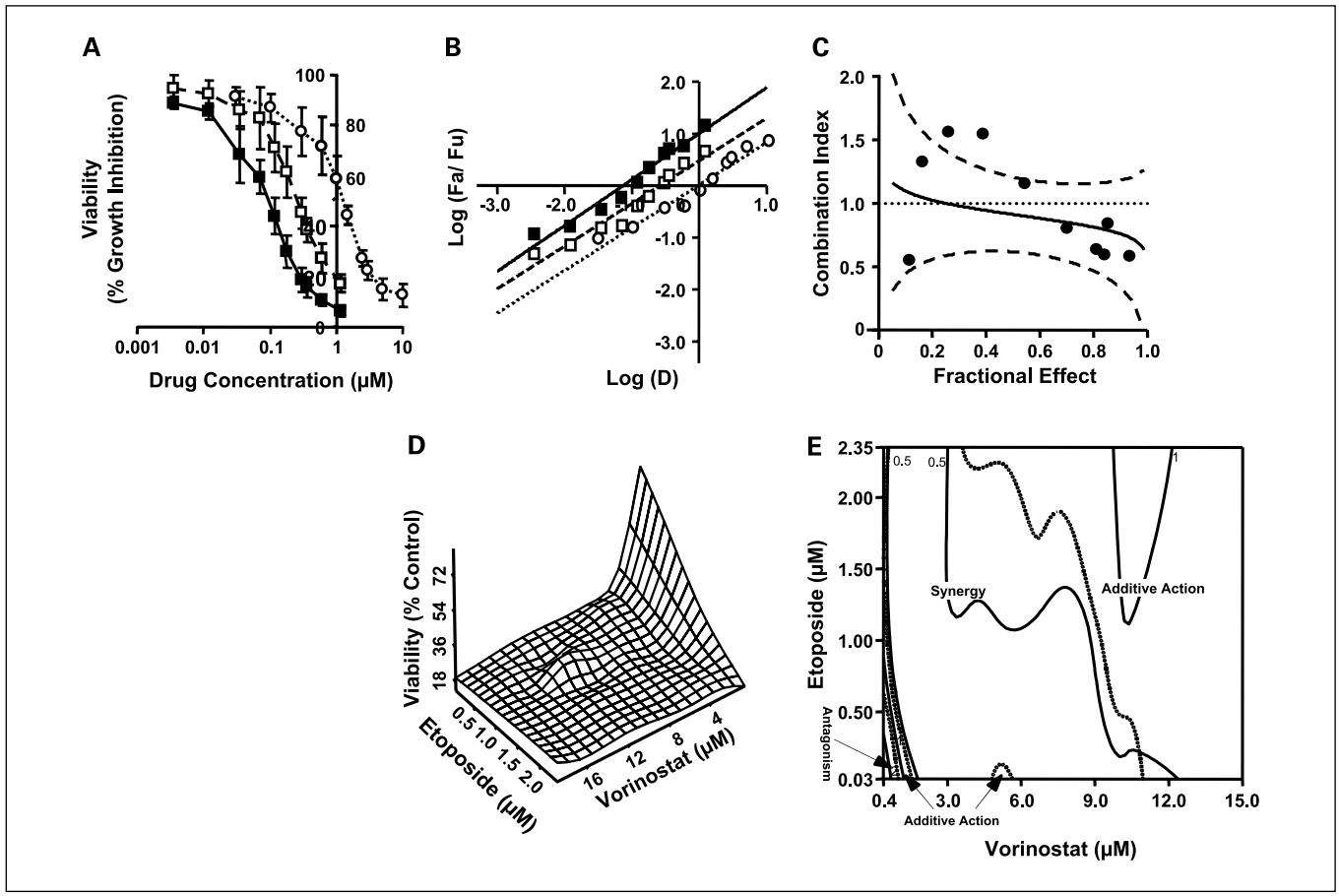

Fig. 5. Simultaneous combination of vorinostat and etoposide results in more-than-additive to synergistic effects. *A,* dose-response curves for growth inhibitory activity of vorinostat alone (○), etoposide alone (□), or the combination (■; at a vorinostat/etoposide ratio of 1.8: 1), measured by the XTT assay. Points, mean for three separate experiments (done on different days), with each data point done in triplicate in each experiment (n = 9); bars, SD. *B,* the CalcuSyn median effect plot for the interaction of the combination of vorinostat with etoposide. Fa, affected fraction; Fu, unaffected fraction. *D,* concentrations of drug used (○, vorinostat alone; □, etoposide alone; ■, the combination). *C,* the combination index plots derived from CalcuSyn software. Dashed lines, 95% confidence intervals; dotted line, combination index = 1. *D,* SynStat maximum power design derived three-dimensional response surface, based on the data from 18 simultaneous combinations of vorinostat and etoposide with four replicates at each combination in HL-60 cells. *E,* the contour plot of the estimated interaction index (τ) surface. The dotted lines are the limits of the 95% confidence interval for additivity.

cells following exposure of cells to a pharmacologically relevant concentration of vorinostat (2.5 μmol/L) may allow us to use this phenomenon to our advantage when vorinostat is used in combination with ara-C.

The interaction between vorinostat and ara-C is sequence dependent. When ara-C was administered to HL-60 cells after vorinostat (vorinostat→ara-C schedule), cytotoxic synergy was observed using both the CalcuSyn and SynStat analytic methods (Fig. 4). As assessed by CalcuSyn (Fig. 4A), the sequential drug schedule produced additive and/or synergistic interactions, particularly at high fractional effect levels. If a drug-free interval was interposed between vorinostat and ara-C exposure (vorinostat→delayed ara-C schedule), the combination index values across all ranges of effect were decreased, particularly with a delay of 72 hours or more after vorinostat exposure. Cells pretreated with vorinostat for 24 hours grew only slightly in the presence of 34.7 nmol/L ara-C (Fig. 4B), and these cell numbers were significantly less than the those for cells treated with vorinostat alone, which showed evidence of regrowth at 196 to 236 hours after the start of the experiment (Fig. 4B).

After identifying the most synergistic sequential combinations using CalcuSyn, we used SynStat to evaluate drug interactions in this sequential schedule. Using 18 optimal mixtures of vorinostat and ara-C with five replicates for each mixture as specified by the SYN.design program, HL-60 cells were exposed first to vorinostat for 24 hours, then placed in drug-free media for 72 hours, after which the appropriate concentrations of ara-C were added for an additional 72 hours. The three-dimensional response surface is shown in Fig. 4C. With the observations from the combination experiments, the F test suggests that vorinostat combined with ara-C against HL-60 is not additive [$F(16, 90) = 16.85$, $P < 0.0001$]. The contour plot of the estimated interaction index (τ) surface showed a synergistic effect across all combinations where the doses of vorinostat were >1 μmol/L, regardless of the dose of ara-C (Fig. 4D). Importantly for clinical translation, when compared with simultaneous exposure (Fig. 1E), no antagonistic effects were noted at low vorinostat concentrations. Taken together, the interaction between vorinostat and ara-C is sequence dependent and can be optimized if vorinostat is given first and followed by ara-C with at least a 72-h drug-free interval.

Combination of vorinostat and etoposide is additive to synergistic, with enhanced synergy in sequential schedule (vorinostat→etoposide). When analyzed by CalcuSyn, the simultaneous combination of vorinostat and etoposide resulted in mostly additive interactions (within the 95% confidence interval for additivity) using the XTT cytotoxicity assay and a fixed vorinostat/etoposide ratio of 8.4:1 (Fig. 5A-C). Similar results were found for this combination using the fluorescein diacetate/propidium iodide method and a fixed vorinostat/etoposide ratio of 5:1, although the combination index values indicated additivity at all effect levels (see Supplementary Fig. S1). Using SynStat (Fig. 5D and E), synergistic interactions were observed at most combinations of drugs, although additive and possibly antagonistic effects can be seen at certain mixtures of vorinostat and etoposide, as can be seen in the contour plot of the estimated interaction index (τ) surface (Fig. 5E). Similar findings were obtained in K562 cells, although the interactions were synergistic at all combinations of vorinostat and etoposide (see Supplementary Fig. S2C and D).

Synergism for combinations of vorinostat and etoposide could be enhanced in HL-60 cells if cells were exposed to vorinostat first, followed by etoposide (Fig. 6). CalcuSyn analysis revealed synergism at higher levels of fractional effect, particularly if the cells were placed in drug-free media for at least 48 hours after exposure to vorinostat, clearly showing improved synergy compared with vorinostat and etoposide given concomitantly (Fig. 6A and B).

Concordant with the CalcuSyn analysis, SynStat maximum power design analysis of HL-60 cells exposed to vorinostat followed by etoposide with a 72-h drug-free interval showed a synergistic effect at most of combinations of vorinostat and etoposide, except where the doses of vorinostat or etoposide were <1.0 μmol/L (Fig. 6C-E).

Discussion

Our studies show the conditions for synergistic interactions between vorinostat and ara-C or etoposide against HL-60

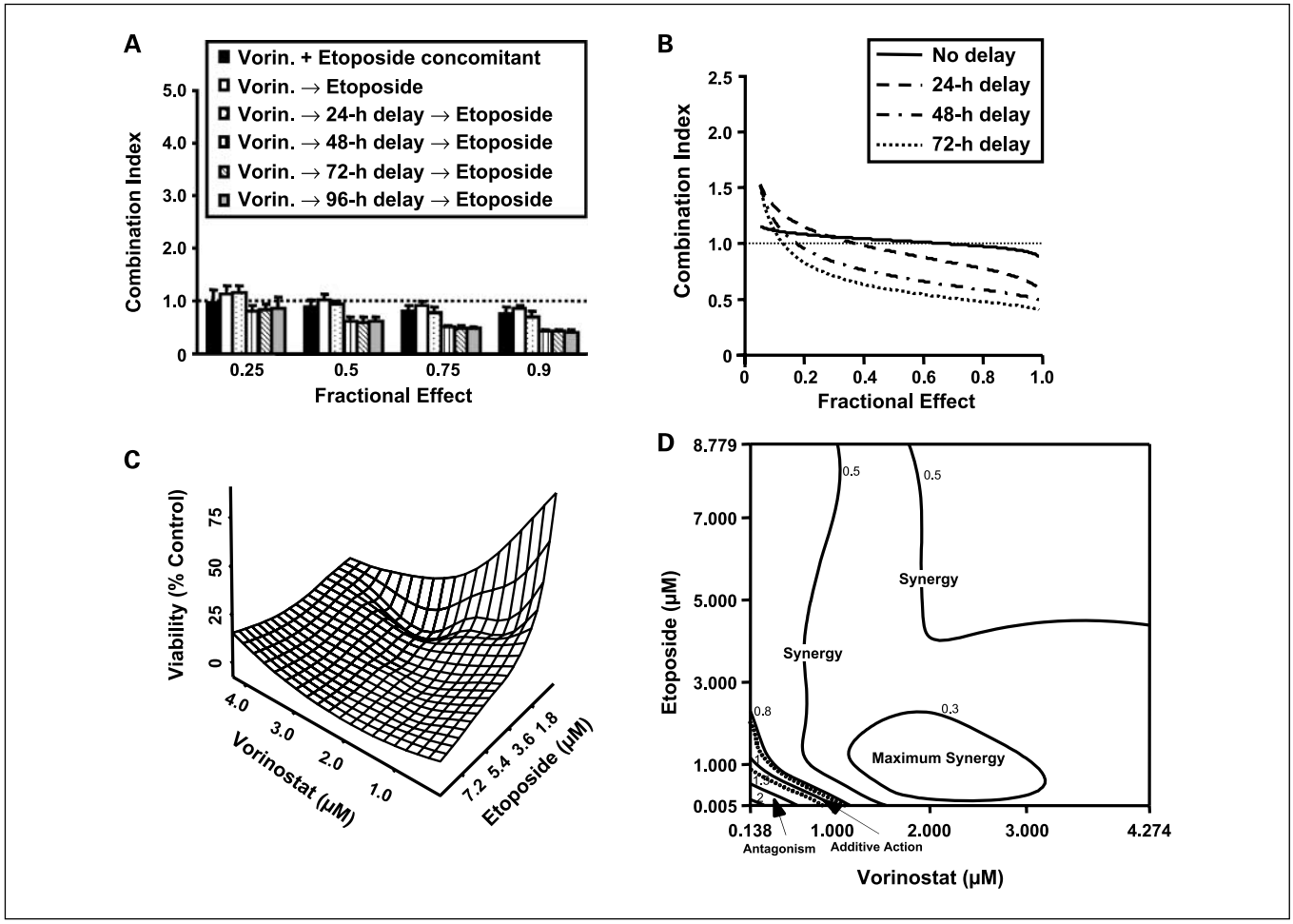

Fig. 6. The interaction between vorinostat and etoposide for the sequential combination. *A,* the combination indices in HL-60 cells are shown for combinations using a 24-h pre-exposure to vorinostat followed by a 72-h exposure to etoposide starting 0 h (*blank*), 24 h (*dot*), 48 h (*stripe*), 72 h (*border*), and 96 h (*shadow*) after removing vorinostat. The combination index values for the interaction are given as a function of the fraction of cells affected. Columns, mean for triplicate experiments, with duplicate data points for each experiment ($n = 6$) for each schedule; bars, SD. Dotted line, combination index = 1. *B,* the combination index plots for each treatment schedule derived from CalcuSyn software. Each line represents mean values ($n = 6$). Dotted line, combination index = 1. *C,* SynStat maximum power design derived three-dimensional response surface, based on the data from 19 sequential combinations of vorinostat and etoposide with five replicates at each combination in HL-60 cells. *D,* the contour plot of the estimated interaction index (τ) surface. The dotted lines indicate the 95% confidence intervals for additivity.

human acute myeloid leukemia cells and K562 chronic myelogenous leukemia blast crisis cells, *in vitro*. Given the ongoing clinical development of vorinostat in early-phase trials, the optimal dose and the timing of administration for vorinostat in combination with antileukemia agents need to be established. Hence, these results provided a rationale for an ongoing clinical trial of vorinostat combined with ara-C and etoposide in acute leukemias.

The synergistic interactions observed occurred at clinically achievable doses of drugs, namely, 0.6 to 5.2 μmol/L for vorinostat and 8.3 to 72 nmol/L for ara-C in the vorinostat + ara-C combination and 0.5 to 3.3 μmol/L for vorinostat and 0.06 to 0.39 μmol/L for etoposide in the vorinostat + etoposide combination (13, 15).

Concomitant administration of vorinostat and ara-C resulted in a less-than-additive or antagonistic effect, whereas sequential administration of vorinostat followed by ara-C was more than additive or synergistic, especially when ara-C was administered several hours after vorinostat (vorinostat→delayed ara-C schedule). Encouraging for clinical translation, an additive or synergistic interaction is observed at nearly all fractional effect levels in the vorinostat→delayed ara-C schedule.

For the combination of vorinostat with etoposide, a more-than-additive to synergistic interaction was seen in the concomitant schedule, with more synergism observed in the sequential vorinostat→etoposide schedule. This sequence dependence is in agreement with studies by Kim et al. (16), showing that combination treatment with vorinostat first was superior to the reverse sequence in human breast cancer cells. Collectively, our findings suggest that vorinostat in combination with ara-C (or etoposide) can be most effective when vorinostat is given first, followed by a drug-free interval, and then followed by ara-C (or etoposide) treatment.

The cytotoxic actions of vorinostat and ara-C we observed seem to be dependent on a cytokinetic effect of pretreatment with vorinostat on cell cycle traverse. We attribute the antagonism observed with the concurrent combination of vorinostat + ara-C to vorinostat causing accumulation of cells in the G_1 or G_2 phase of the cell cycle, thus blocking S-phase entry and abrogating ara-C cytotoxicity because ara-C is dependent on DNA synthesis for its cytotoxic action. Similarly, recovery of the proportion of cells entering S phase following vorinostat exposure may provide the basis for the synergism observed in the vorinostat followed by ara-C schedules. These alternations of cell cycle kinetics caused by vorinostat are consistent with those reported in human breast cancer cell lines by Munster et al. (33), in which they found that 48-hour exposure to 2.5 and 5 μmol/L of vorinostat accumulated G_1-phase cells and this was reversible within 48 hours after the removal of vorinostat.

Our observation of a synergistic interaction between vorinostat and etoposide might also be due to cell cycle alterations because etoposide is also known to be a phase-specific drug, acting in the late S phase of the cell cycle (28). Nevertheless, it might be possible that etoposide is working under cell cycle–independent mechanisms of action because etoposide can kill cells to some extent at all phases of the cell cycle (28, 29). Furthermore, recent reports suggest cell cycle–independent mechanisms for synergistic interactions between vorinostat and topoisomerase II inhibitors. Kim et al. (16) postulated the cytotoxic synergy between vorinostat and etoposide to be due to the opening of the chromatin structure allowing better accessibility of DNA to etoposide. More recently, Marchion et al. (34) reported that pre-exposure to vorinostat caused a structural change in the chromatin with an increased association of epirubicin with DNA. Accordingly, vorinostat might have additional novel mechanisms of action other than affecting cell cycle that sensitize the cells to etoposide, making it promising to administer in sequential combination for clinical benefit. Interestingly, Johnson et al. (35) reported that pretreatment with another histone deacetylase inhibitor trichostatin A suppressed etoposide-mediated apoptosis in a variety of cell lines, including HL-60. This study used a small nontoxic dose of trichostatin A (0.1 μmol/L) before treatment with a large dose of etoposide (100 μmol/L). In agreement, our model could show that vorinostat and etoposide combinations resulted in antagonism in certain combinations, namely, at lower doses of vorinostat where a lower level of effect was seen (Figs. 5 and 6).

CalcuSyn software defines the combination index based on the median effect and the assumption that each drug and their combinations have a log-linear dose-response with a constant relative potency. In addition, the combination index stays the same for any combinations within a fixed dose ratio. As pointed out by Greco et al. (ref. 36, p. 380), both the inherent nonlinear nature of the median effect plot and the incorrect calculation of the combination index for the case of mutual nonexclusivity contribute to incorrect and artifactual conclusions on synergism and antagonism when applying the CalcuSyn method of Chou and Talalay (24) to different laboratory data. Because the experiments for single agents showed that the relative potency between vorinostat and ara-C or etoposide is not constant, we found it useful to use SynStat (which does not assume constant relative potency) in addition to CalcuSyn. SynStat assumes neither constant relative potency nor any parametric forms of joint action. It allows exploration of all the levels of joint effects (as opposed to considering the median effect alone, as does CalcuSyn). The work presented here shows congruency of the two methods of assessing drug interaction; however, the ability of SynStat to display the interaction effect (synergy, additivity, or antagonism) represented by τ in a contour plot as a function of the concentrations of each drug studied allows for more facile appreciation of what concentrations of each drug in a mixture result in synergy, additivity, or antagonism.

In summary, our studies show that vorinostat can enhance the cytotoxicity of ara-C or etoposide in human leukemia cell lines, particularly when vorinostat is given before ara-C or etoposide. Furthermore, we find it likely that vorinostat-related cell cycle perturbations could play a role in potentiating the cytotoxic interaction of both drugs. Finally, we designed a sequential drug exposure scheme to allow time for surviving cells in G_1- or G_2-phase arrest after vorinostat exposure to reenter S phase and thereby acquire sensitivity to ara-C. Although we cannot exclude the possibility that vorinostat and ara-C (or etoposide) are interacting through mechanisms other than cell cycle kinetics, we observed an apparent advantage of sequential vorinostat combinations with delayed ara-C and/or etoposide over either agent given singly, both agents simultaneously, or vorinostat followed immediately by ara-C (or etoposide). Our data, therefore, provide the framework for future clinical evaluations of combination regimens of vorinostat with ara-C and/or etoposide. Phase I clinical studies

have shown that oral vorinostat can be administered with demonstrable biological activity (13), as evidenced by histone acetylation in peripheral mononuclear cells (2, 37). The concentrations of histone deacetylase inhibitors that are required for cell cycle arrest are known to correlate with those required to cause accumulation of acetylated histones (2). Accordingly, we have begun a phase I clinical trial of oral vorinostat followed by ara-C and etoposide in patients with relapsed or refractory acute leukemias.

Disclosure of Potential Conflicts of Interest

D. Ross has received a commercial research grant from Merck to support translational work for a clinical trial.

Acknowledgments

We thank Dr. James Zwiebel of the Cancer Therapy Evaluation Program of the National Cancer Institute for his helpful suggestions with regard to these studies.

References

1. Jemal A, Murray T, Ward E, et al. Cancer statistics, 2005. CA Cancer J Clin 2005;55:10–30.
2. Richon VM, Emiliani S, Verdin E, et al. A class of hybrid polar inducers of transformed cell differentiation inhibits histone deacetylases. Proc Natl Acad Sci U S A 1998;95:3003–7.
3. Richon VM, Webb Y, Merger R, et al. Second generation hybrid polar compounds are potent inducers of transformed cell differentiation. Proc Natl Acad Sci U S A 1996;93:5705–8.
4. Finnin MS, Donigian JR, Cohen A, et al. Structures of a histone deacetylase homologue bound to the TSA and SAHA inhibitors. Nature 1999;401:188–93.
5. Johnstone RW, Licht JD. Histone deacetylase inhibitors in cancer therapy: is transcription the primary target? Cancer Cell 2003;4:13–8.
6. Marks PA, Rifkind R, Richon VM, et al. Histone deacetylases and cancer: causes and therapies. Nat Rev Cancer 2001;1:194–202.
7. Amin HM, Saeed S, Alkan S. Histone deacetylase inhibitors induce caspase-dependent apoptosis and downregulation of daxx in acute promyelocytic leukaemia with t(15;17). Br J Haematol 2001;115:287–97.
8. Mitsiades N, Mitsiades CS, Richardson PG, et al. Molecular sequelae of histone deacetylase inhibition in human malignant B cells. Blood 2003;101:4055–62.
9. Nimmanapalli R, Fuino L, Stobaugh C, et al. Cotreatment with the histone deacetylase inhibitor suberoylanilide hydroxamic acid (SAHA) enhances imatinib-induced apoptosis of Bcr-Abl-positive human acute leukemia cells. Blood 2003;101:3236–9.
10. Sakajiri S, Kumagai T, Kawamata N, et al. Histone deacetylase inhibitors profoundly decrease proliferation of human lymphoid cancer cell lines. Exp Hematol 2005;33:53–61.
11. Vrana JA, Decker RH, Johnson CR, et al. Induction of apoptosis in U937 human leukemia cells by suberoylanilide hydroxamic acid (SAHA) proceeds through pathways that are regulated by Bcl-2/Bcl-XL, c-Jun, and p21CIP1, but independent of p53. Oncogene 1999;18:7016–25.
12. Yu C, Rahmani M, Almenara J, et al. Histone deacetylase inhibitors promote STI571-mediated apoptosis in STI571-sensitive and -resistant Bcr/Abl$^+$ human myeloid leukemia cells. Cancer Res 2003;63:2118–26.
13. Kelly WK, O'Connor OA, Krug LM, et al. Phase I study of an oral histone deacetylase inhibitor, suberoylanilide hydroxamic acid, in patients with advanced cancer. J Clin Oncol 2005;23:3923–31.
14. Kelly WK, O'Connor OA, Marks PA. Histone deacetylase inhibitors: from target to clinical trials. Expert Opin Investig Drugs 2002;11:1695–713.
15. Kelly WK, Richon VM, O'Connor O, et al. Phase I clinical trial of histone deacetylase inhibitor: suberoylanilide hydroxamic acid administered intravenously. Clin Cancer Res 2003;9:3578–88.
16. Kim MS, Blake M, Baek JH, et al. Inhibition of histone deacetylase increases cytotoxicity to anticancer drugs targeting DNA. Cancer Res 2003;63:7291–300.
17. Di Gennaro E, Bruzzese F, Romano G, et al. Antitumor effect of histone deacetylase inhibitor SAHA alone and combined with cytotoxic drugs in human colorectal cancer cells. Proc Am Assoc Cancer Res 2003;44:724 (abstract 3636).
18. Almenara J, Rosato R, Grant S. Synergistic induction of mitochondrial damage and apoptosis in human leukemia cells by flavopiridol and the histone deacetylase inhibitor suberoylanilide hydroxamic acid (SAHA). Leukemia 2002;16:1331–43.
19. Gao N, Dai Y, Rahmani M, et al. Contribution of disruption of the nuclear factor-κB pathway to induction of apoptosis in human leukemia cells by histone deacetylase inhibitors and flavopiridol. Mol Pharmacol 2004;66:956–63.
20. Zhu WG, Otterson GA. The interaction of histone deacetylase inhibitors and DNA methyltransferase inhibitors in the treatment of human cancer cells. Curr Med Chem Anti-Canc Agents 2003;3:187–99.
21. Yu C, Rahmani M, Conrad D, et al. The proteasome inhibitor bortezomib interacts synergistically with histone deacetylase inhibitors to induce apoptosis in Bcr/Abl$^+$ cells sensitive and resistant to STI571. Blood 2003;102:3765–74.
22. He LZ, Tolentino T, Grayson P, et al. Histone deacetylase inhibitors induce remission in transgenic models of therapy-resistant acute promyelocytic leukemia. J Clin Invest 2001;108:1321–30.
23. Chou TC. The median-effect principle and the combination index for quantitation of synergism and antagonism. In: Chou TC, Rideout DC, editors. Synergism and antagonism in chemotherapy. San Diego: Academic Press; 1991. p. 61–102.
24. Chou TC, Talalay P. Quantitative analysis of dose-effect relationships: the combined effects of multiple drugs or enzyme inhibitors. Adv Enzyme Regul 1984;22:27–55.
25. Fang HB, Ross DD, Sausville E, et al. Experimental design and interaction analysis of combination studies of drugs with log-linear dose responses. Stat Med 2008;27:3071–83.
26. Tan M, Fang HB, Tian GL, et al. Experimental design and sample size determination for testing synergism in drug combination studies based on uniform measures. Stat Med 2003;22:2091–100.
27. Meyn RE, Meistrich ML, White RA. Cycle-dependent anticancer drug cytotoxicity in mammalian cells synchronized by centrifugal elutriation. J Natl Cancer Inst 1980;64:1215–9.
28. Chow KC, Ross WE. Topoisomerase-specific drug sensitivity in relation to cell cycle progression. Mol Cell Biol 1987;7:3119–23.
29. Nitiss JL, Wang JC. Mechanisms of cell killing by drugs that trap covalent complexes between DNA topoisomerases and DNA. Mol Pharmacol 1996;50:1095–102.
30. Ross DD, Joneckis CC, Ordonez JV, et al. Estimation of cell survival by flow cytometric quantification of fluorescein diacetate/propidium iodide viable cell number. Cancer Res 1989;49:3776–82.
31. Berenbaum MC. Synergy, additivism and antagonism in immunosuppression. A critical review. Clin Exp Immunol 1977;28:1–18.
32. Marks P, Rifkind RA, Richon VM, et al. Histone deacetylases and cancer: causes and therapies. Nat Rev Cancer 2001;1:194–202.
33. Munster PN, Troso-Sandoval T, Rosen N, et al. The histone deacetylase inhibitor suberoylanilide hydroxamic acid induces differentiation of human breast cancer cells. Cancer Res 2001;61:8492–7.
34. Marchion DC, Bicaku E, Daud AI, et al. Sequence-specific potentiation of topoisomerase II inhibitors by the histone deacetylase inhibitor suberoylanilide hydroxamic acid. J Cell Biochem 2004;92:223–37.
35. Johnson CA, Padget K, Austin CA, et al. Deacetylase activity associates with topoisomerase II and is necessary for etoposide-induced apoptosis. J Biol Chem 2001;276:4539–42.
36. Greco WR, Bravo G, Parsons JC. The search for synergy: a critical review from a response surface perspective. Pharmacol Rev 1995;47:331–85.
37. Marks PA, Rifkind RA, Richon VM, et al. Inhibitors of histone deacetylase are potentially effective anticancer agents. Clin Cancer Res 2001;7:759–60.